Available online at www.sciencedirect.com

ScienceDirect

Ceramics International 40 (2014) 3379–3388

CERAMICS INTERNATIONAL

www.elsevier.com/locate/ceramint

Rietveld refinement of hydroxyapatite, tricalcium phosphate and biphasic materials prepared by solution combustion method

Junfeng Zhao[a,b,*], Junjie Zhao[a], JianHua Chen[a,b], XuHong Wang[a,b], Zhida Han[a,b], Yuhong Li[a,b]

[a]College of Material Science and Engineering, Changshu Institute of Technology, Changshu 215500, China
[b]Jiangsu Laboratory of Advanced Functional Materials, Changshu Institute of Technology, Changshu 215500, China

Received 14 November 2012; received in revised form 11 September 2013; accepted 21 September 2013
Available online 27 September 2013

Abstract

The solution combustion method was used to prepare single phase hydroxyapatite (HA), β-tricalcium phosphate (β-TCP) and biphasic calcium phosphates (BCP). The powder samples were synthesized with a Ca/P molar ratio from 1.45 to 1.67, and annealed at different temperatures. These samples have been characterized by XRD and FTIR. The amount and lattice parameters of each phase in these samples were refined by the MAUD program. The results of Rietveld refinement show that a single phase HA is obtained with Ca/P ratio of 1.67 and annealing at 1150 °C for 3 h, β-TCP is isolated with a Ca/P ratio of 1.5 after annealing at 950 °C and remains stable up to 1050 °C. Apart from above two extremes a whole range of BCP can be prepared with a favorable control of Ca/P ratios and annealing temperatures.

Keywords: B. X-ray methods; Biphasic tricalcium phosphate; Solution combustion method; Rietveld refinement

1. Introduction

Synthetic hydroxyapatite (HA) and tricalcium phosphate (TCP) have been recognized as the most important biomaterial for their bioactivity and osteoconductive properties in vivo [1–4]. Recently, many studies have focused on potential application in the fields of bioceramics and bone cement. However, both materials show a number of drawbacks that reduce their clinical performances. The dissolution of HA in the human body after implantation is too low to achieve the optimal formation of bone tissue. On the other hand, β-TCP shows fast release of Ca^{2+} and PO_4^{3-} ions when exposed to physiological fluids [5], and the degradation rate of β-TCP is 10 times higher than that of HA [6]. These results motivated growing interest in developing BCP consisting of HA and β-TCP has better osteoinduction than single phasic HA and β-TCP due to its controllable degradation rate and more effective bone regeneration ability [7]. Generally, BCP can be prepared by mechanical mixing of HA and β-TCP [8] or through decomposition of calcium-deficient hydroxyapatite (CDHA) by sintering above 700 °C [9,10]. The second procedure seems to be better because the mixture of phases on the atomic level leads to an increased purity, conserved bioactive and biodegradable properties and better mechanical characteristics [11], as well as an improved sintering behavior [12,13]. CDHA possessing the Ca/P ratio varying between 1.67 and 1.5 leads to the formation of biphasic mixture of HA and β-TCP when annealed above 700 °C [14]:

$$Ca_{10-x}(HPO_4)_x(PO_4)_{6-x}(OH)_{2-x} \rightarrow (1-x)Ca_{10}(PO_4)_6OH + 3xCa_3(PO_4)_2 + xH_2O \quad (1)$$

In addition, many synthesis methods have been reported for synthesizing BCP, such as precipitation [15,16], sol–gel [17], microwave [18,19], liquid mix techniques [20],spray pyrolysis [21], treatment of nature bone [22,23] and combustion processing [24]. The self-propagating combustion synthesis (SPCS) is an effective, low-cost method for the production of various industrially useful materials [25]. Currently, submicron sized calcium phosphate (HA and β-TCP) could be synthesized by SPCS [26]. Moreover, the effects of different fuels and fuel

*Corresponding author at: College of Material Science and Engineering, Changshu Institute of Technology, Changshu 215500, China.
Tel./fax: +86 512 52251842.
E-mail address: daidai02304@163.com (J. Zhao).

0272-8842/$ - see front matter © 2013 Elsevier Ltd and Techna Group S.r.l. All rights reserved.
http://dx.doi.org/10.1016/j.ceramint.2013.09.094

ratios on the phase formation of different calcium phosphates bioceramics also have been considered [24–31]. However, not enough attention has been paid to control the different proportions of biphasic β-TCP/HA materials.

The purpose of this study was to prepare single phase HA, β-TCP and BCP by the solution combustion method with addition of the combustion aid (NH_4NO_3) to control the intensity of reaction. In addition, a whole range of BCP were prepared with a favorable control of Ca/P molar ratios ($1.45 \leq Ca/P \leq 1.67$) and annealing temperature(from 750 to 1150 °C).

2. Experimental

2.1. Sample preparation

The flowchart for preparing single-phase HA, TCP and BCP by the solution combustion method is shown in Fig. 1. The raw materials included $Ca(NO_3)_2 \cdot 4H_2O$, $NH_4H_2PO_4$, $C_6H_8O_7$ and NH_4NO_3 with analytical grade. The reactants were calculated based on the Ca/P molar ratio of 1.45, 1.5, 1.525, 1.55, 1.575, 1.6, 1.625, 1.65 and 1.67. The molar ratio of $C_6H_8O_7$ and $Ca(NO_3)_2 \cdot 4H_2O$ was kept constant at 1. $NH_4NO_3/Ca(NO_3)_2 \cdot 4H_2O$ (molar ratio) was varied between 1 and 6 with fixed Ca/P ratio at 1.67. Firstly, stoichiometric ratio of $Ca(NO_3)_2 \cdot 4H_2O$ citric acid and $NH_4H_2PO_4$ were dissolved in deionized water at room temperature. Different proportions of ammonium nitrate were added to improve the combustion intensity. The mixture was evaporated at 80 °C until it formed the colloidal solution. Then, the colloidal solution swelled rapidly and revealed a vigorous self-propagating combustion reaction. The fluffy product was obtained after cooling down at room temperature in air. Finally, the samples were annealed accumulatively from 750 to 1150 °C for 3 h.

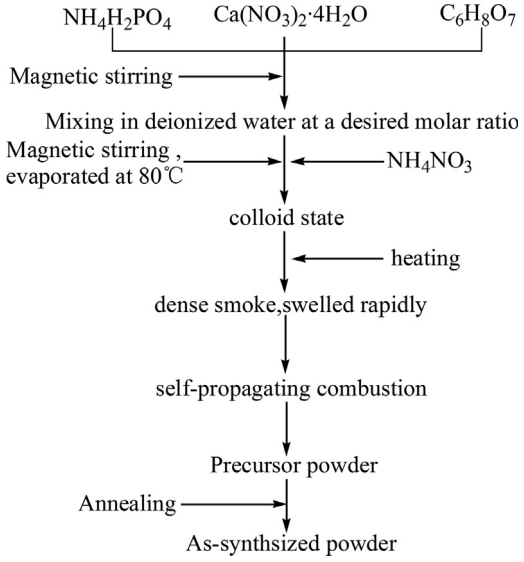

Fig. 1. The flowchart for preparing powder by solution combustion method.

2.2. Power characterization

The crystal structure was described by X-ray diffraction (Dmax-2200PC) with CuKα radiation (40 KV, 40 mA) and step size of 0.02° and a present time of 4 s. Fourier transform Infrared (IR) spectroscopy (Nicolet 380) was carried out at room temperature in the range of 400–4000 cm^{-1} using samples in the form of pellets formed with spectroscopic grade KBr. The Rietveld analysis was performed on the diffraction patterns using the program MAUD. It applied the RITA/RISTA method as developed by Ferrari and Lutterotti [32]. The program was developed to analyze diffraction spectra and obtained crystal structures, amount and microstructure of phase along with the texture and residual stresses [33,34]. Another significant advantage of using the MAUD program is in the estimation of the particle size distribution according to the lognormal distribution model proposed by Popa and Balzar [36].

3. Results and discussion

3.1. Effect of the NH_4NO_3

In this study, citric acid was jointly used as the fuel, while ammonium nitrate (NH_4NO_3) was introduced as the combustion aid for low-temperature synthesis [37]. The synthesis with NH_4NO_3 addition has double functions, which helps to enhance the intensity of combustion and in the formation of the porous network structure as the decomposition of NH_4NO_3 releases gasses, such as NH_3, NO_x and H_2O [38]. Table 1 represents the combustion status and powder state with the different molar ratios of NH_4NO_3/metal nitrate (N/M = 0, 1, 2, 3, 4, 5, 6). The acuteness degree of combustion was enhanced with the increase of N/M ratio. However, the powder was difficult to collect when N/M ratio reached 6, which can be ascribed to energy loss and a lower combustion temperature with the amount of generated gasses increasing. Fig. 2 shows

Table1
The combustion status and appearance of product with addition of NH_4NO_3.

Sample ID	Quality ratio of $NH_4NO_3/Ca(NO3) \cdot 4H2O$	Combustion status	Appearance of product
N/M = 0	0	Smoldering	Black, agglomerate
N/M = 1	1	Imperfect	Black, agglomerate
N/M = 2	2	sufficient	Black, Slightly fluffy
N/M = 3	3	sufficient	Gray, Slightly fluffy
N/M = 4	4	Violent	Gray, fluffy
N/M = 5	5	Violent	White, fluffy
N/M = 6	6	Dense smoke	Gray, difficult to collect

Fig. 2. The appearance of the products before annealing.

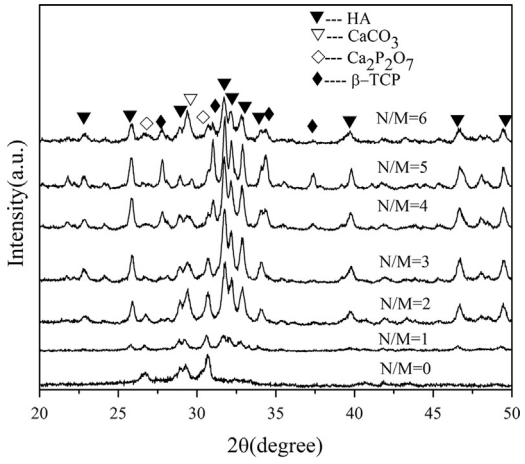

Fig. 3. XRD patterns of the synthesized powders obtained from systems containing different amounts of NH_4NO_3 (Ca/P = 1.67).

the appearance of the sample (Ca/P = 1.67) before annealing. A white mass was obtained as a combustion product, which appeared as a sponge structure.

3.2. Analysis of phase compositions

Fig. 3 shows the XRD spectra of the samples obtained with different N/M ratios. Samples prepared without addition of NH_4NO_3 show the presence of γ-$Ca_2P_2O_7$ (Powder Diffraction File 17-499 JCPDS 2000) and $CaCO_3$ (Powder Diffraction File 5-586 JCPDS 2000). For N/M = 1, the HA (Powder Diffraction File 9-432 JCPDS 2000) phases start to form. With the increase of NH_4NO_3 content, the diffraction intensity of γ-$Ca_2P_2O_7$ and $CaCO_3$ reduced, the β-TCP (Powder Diffraction File 9-169 JCPDS 2000) phases formed at N/M = 4, and further increased at N/M = 5. Thus, the changes of the N/M ratio were found to provide a useful control in the final phase assemblage. In order to ensure that the bi-phasic structure is formed well, all the samples in the following comparative studies were focused on these precursors with N/M values fixed at 5.

Fig. 4 shows the XRD spectra of the samples synthesized with different temperatures. Regarding the first point, a Ca/P ratio of 1.5 leads to the formation of β-TCP shown in Fig. 4(a), sample with annealing at 750 °C shows the presence of β-$Ca_2P_2O_7$ (Powder Diffraction File 9-346 JCPDS 2000) and $CaCO_3$, these two phases translated into β-TCP with the increase of temperatures. The biphasic material obtained after annealing at 850 °C, and turned into relatively pure β-TCP phase at 950 °C. This transition has been described to occur at about 1100 °C [20,39]. In addition, a small amount of α-TCP and HA phase appeared in the XRD pattern when the temperature reached 1150 °C. Samples synthesized with Ca/P ratio of 1.575 all produced bi-phasic mixtures of HA and β-TCP, Fig. 4(b) represents the phase transformation process of the compositions. The diffraction intensity of β-TCP phase attained its maximum at 850 °C, and then gradually decreased from 950 °C to 1150 °C. Similarly, the highest intensity of β-TCP phase appeared at 850 °C with Ca/P ratio of 1.67, and the β-TCP phase translated into HA with increasing of temperature, single-phase HA formed at 1150 °C [Fig. 4(c)].

Fig. 5 shows the XRD spectra of the powder samples synthesized with different Ca/P ratios. The samples of this figure were all annealed in air at 1150 °C for 3 h. The variations in the nominal Ca/P ratio were found to provide a favorable control in the final phase assemblage. Single-phase HA and β-TCP phases were obtained when Ca/P (molar) ratios were 1.67 and 1.45 respectively. Samples at $1.5 \leq Ca/P \leq 1.65$ all produced two main phases of HA and β-TCP. The diffraction intensity of HA in the mixtures enhanced with increase of Ca/P ratio. Thus, the combustion method can be regarded as an efficient way to produce single-phase HA, TCP, bi-phasic mixture of HA and TCP.

3.3. Rietveld refinement results

Quantitative phase analyses were extracted from Rietveld refinements. Rietveld refinement was performed using the structural models (ISCD database) of all possible occurring secondary phases listed in Table 2. Fig. 6 collects the resulting plot of Rietveld analysis effectuated on the 1.67, 1.575 and 1.5 samples. Refined mineralogical compositions of the samples are listed in Table 3 and 4. Fig. 7 shows the thermal evolution of the samples synthesized with Ca/P ratio of 1.5, 1.575 and 1.67. HA and β-TCP wt% show opposite evolution. The curves present a similar trend when the Ca/P ratio were 1.575 and 1.67, a least amount of HA phase for the sample heat treated at 850 °C (33.87% at 1.575, 48.75% at 1.67), then the amount of HA increased when the temperature increases from 850 °C to 1150 °C. β-TCP was the major phase when Ca/P ratio was 1.5, the weight percent of β-TCP increased from 750 °C to 1050 °C to reach a large majority of 99.19%,

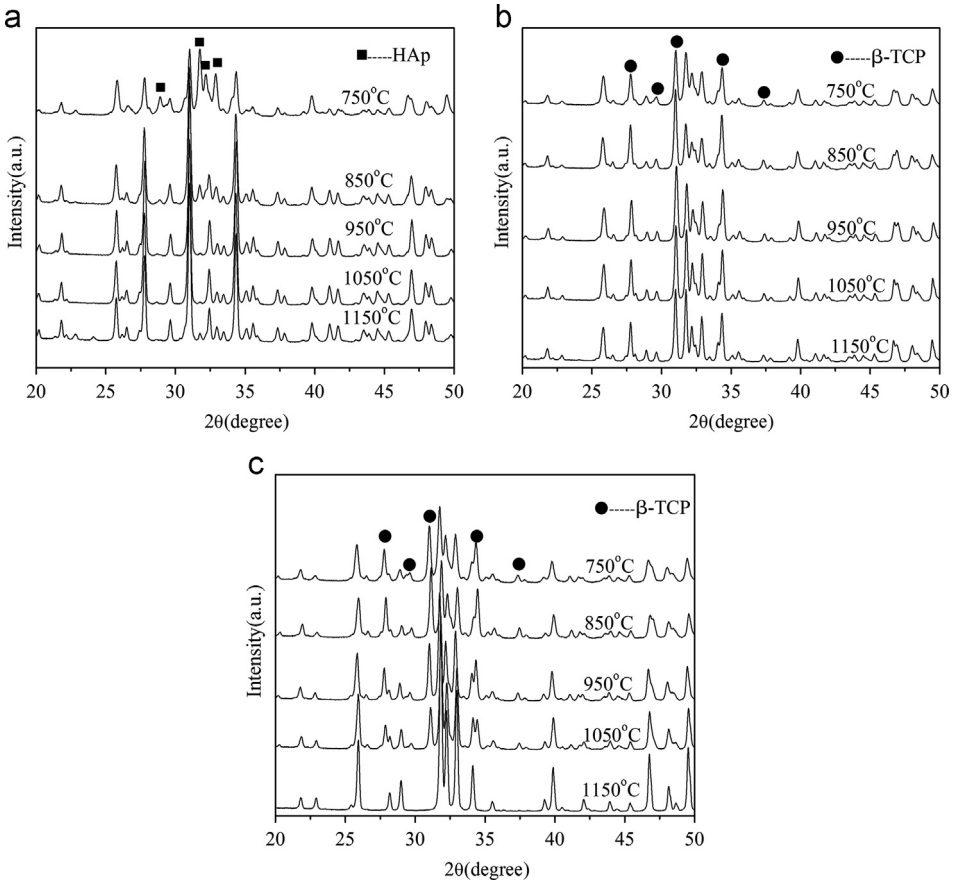

Fig. 4. XRD patterns of the powders synthesized with different temperatures (a) Ca/P=1.5, (b) Ca/P=1.575, and (c) Ca/P=1.67.

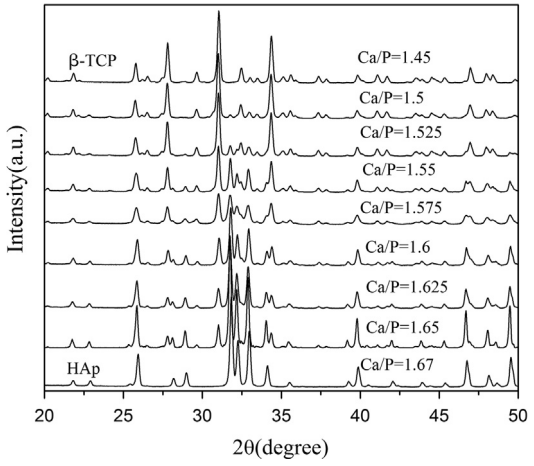

Fig. 5. XRD patterns of the powders synthesized with different Ca/P ratios (1150 °C, air, 3 h).

then slightly decreased at 1150 °C. A small amount of CaCO3 and CaO appeared in most of the products (Table 3). Overall, the above two phase decreased with increase of annealing temperature. In addition, trace of α-TCP formed at 1150 °C (5.40% at 1.5, 0.58% at 1.575). These results indicate that single phase HA is obtained with Ca/P ratio of 1.67 after annealing at 1150 °C, while β-TCP is isolated with a Ca/P ratio of 1.5 after annealing at 950 °C and remains stable up to 1050 °C in this method.

Table 2
The structural models (ISCD Database) of all possible occurring secondary phases

Phase		Structural model	
Name	Formula	ICSD code	Reference
HAP(hydroxyapatite)	Ca5(PO4)3(OH)	56306	[40]
β-TCP(whitlockite)	Ca3P2O8	97500	[41]
α-TCP	Ca3P2O8	923	[42]
β-C2P	Ca2P2O7	73712	[43]
Calcium carbonate	CaCO3	40107	[44]
Calcium oxide	CaO	52783	[45]

Fig. 8 shows quantitative phase analyses of the samples prepared with different Ca/P ratio and annealed at 1150 °C. The progressive transformation of HA content was expressed in Fig. 8(a), the samples obtained by this method shows a reasonable accordance with the theoretical amount of HA in the mixture. Fig. 8(b) shows a comparison between the results determined by XRD and chemical titration, these results show a correspondence with the theoretical Ca/P ratio. As shown in Fig. 8(c), the amount of α-TCP expresses approximate linear

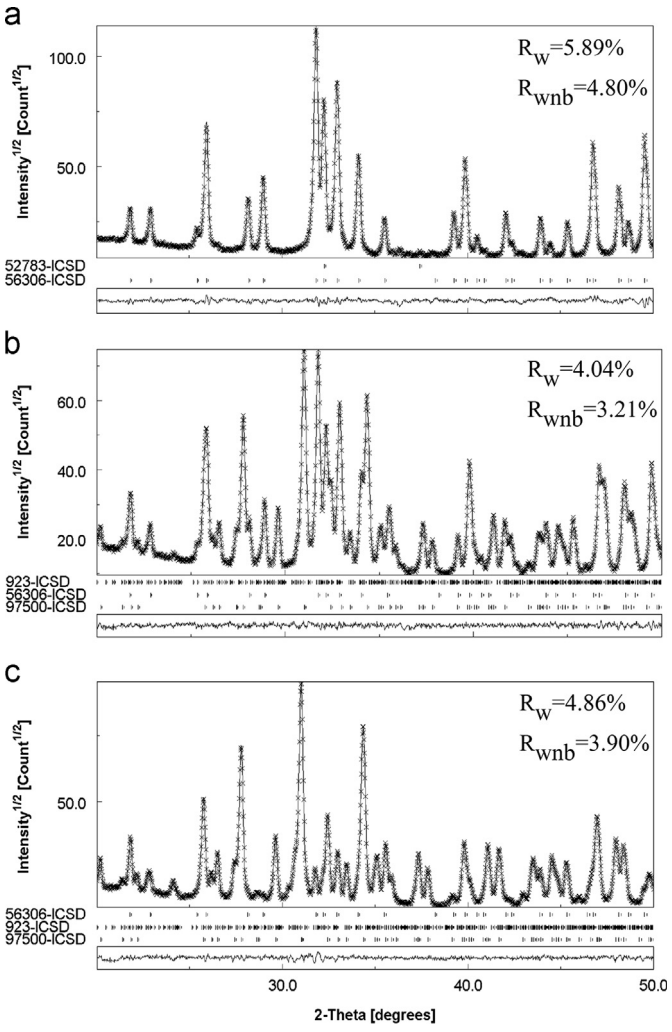

Fig. 6. Rieteveld refinement for selected samples annealing at 1150 °C: (a) Ca/P=1.67; (b) Ca/P=1.575; and (c) Ca/P=1.5.

decline with the increase of Ca/P ratios ($1.5 \leq Ca/P \leq 1.6$). Consequently, these data justify this method as an efficient way to produce biphasic materials with controllable proportion of each phase.

Table 5 shows the unit cell parameters for whole samples. The lattice parameters of the HA phase in the composite powder samples prepared with different Ca/P ratios remained almost constant [Fig. 9(a)], while the lattice parameters of the β-TCP phase displayed almost decreased with the increase of Ca/P ratios [Fig. 9(b)]. These results were consistent with the data from Tas et al. [46]. Remarkably, Fig. 9(c) and (d) presents the effect of annealing temperature on the lattice parameters of HA and β-TCP for different powder compositions investigated. Over the investigated range of temperatures, all the powders show a relatively uniform trend in the variation in *α*-axis and *c*-axis parameter values. To be precise, almost all of the compositions show higher *α*-axis and *c*-axis parameter values of HA and β-TCP at 850 °C, and then decreased with the temperature increased from 850 °C to 1050 °C. It might be ascribed to carbonated substitutions from decomposition of calcium carbonate [47].

3.4. FTIR analysis

FTIR spectra displayed in Fig. 10 also confirm the relevance of phase transformation from β-TCP to HA for samples synthesized with different Ca/P ratios, and the mine bands and their characteristics are listed in Table 6. The characteristic bands for PO_4^{3-} appeared at 1121, 1043, 969, 944, 604 and 552 cm^{-1} corresponded to β-TCP structure [48,49]. The bands at 1121 and 1043 cm^{-1} corresponded to the ν_3 vibration of PO_4^{3-} ions. The bands at 969 and 1043 cm^{-1} were assigned to the ν_1 vibration of the O–P–O mode, and the peaks at 604 and 552 cm^{-1} were

Table 3
Results of the quantitative (wt%) extracted from Rietveld refinements annealing at different temperature.

Ca/P ratio	T/°C	Mineralogical composition (wt%)						Rw (%)	Rwnb (%)
		HA	β-TCP	α-TCP	CaCO3	CaO	Ca2P2O7		
1.5	750	33.17(2)	43.81(6)	–	14.84(2)	3.78(5)	4.40(3)	9.09	8.57
	850	11.16(7)	85.77(1)	–	1.50(3)	–	1.57(3)	4.99	3.77
	950	0.67(7)	99.18(7)	–	–	0.13(2)	0.02(3)	4.30	3.29
	1050	0.81(3)	99.19(6)	–	–	–	–	4.93	3.94
	1150	3.21(9)	91.39(5)	5.40(4)	–		–	4.86	3.90
1.575	750	47.93(1)	50.80(2)	–	1.13(9)	0.14(6)	–	4.43	3.27
	850	33.87(5)	64.87(2)	–	0.30(8)	0.96(3)	–	3.63	2.79
	950	38.87(1)	57.91(7)	–	0.24(1)	3.88(3)	–	3.72	2.71
	1050	42.60(6)	57.25(1)	–	–	0.15(2)	–	5.33	4.57
	1150	43.14(8)	55.63(4)	1.23(6)	–	–	–	4.04	3.21
1.67	750	55.86(7)	41.59(8)	–	1.79(7)	0.77(6)	–	3.89	3.08
	850	48.75(3)	49.45(5)	–	1.12(1)	0.68(9)	–	4.37	3.14
	950	63.75(3)	34.79(8)	–	0.83(1)	0.63(7)	–	4.23	3.19
	1050	68.45(6)	30.49(3)	–	0.45(6)	0.61(2)	–	4.48	3.49
	1150	99.92(1)	–	–	–	0.08(9)	–	5.89	4.80

Table 4
Results of the quantitative (wt%) extracted from Rietveld refinements with different Ca/P ratio.

Ca/P ratio	T/°C	Mineralogical composition (wt%)					Rw (%)	Rwnb (%)
		HA	β-TCP	α-TCP	CaO	$Ca_2P_2O_7$		
1.45	1150	–	95.64(3)	–	–	4.36(4)	6.23	4.55
1.5	1150	3.21(9)	91.39(5)	5.40(4)	–	–	4.83	3.95
1.525	1150	9.29(7)	88.05(1)	2.66(1)	–	–	4.91	4.10
1.55	1150	36.05(3)	61.82(1)	2.23(1)	–	–	5.12	4.08
1.575	1150	43.22(8)	56.20(4)	0.58(1)	–	–	4.45	3.37
1.6	1150	62.04(1)	37.5(4)	0.46(1)	–	–	4.54	3.60
1.625	1150	73.69(3)	26.31(9)	–	–	–	4.69	3.64
1.65	1150	82.62(7)	17.38(2)	–	–	–	4.51	3.54
1.67	1150	99.92(1)	–	–	0.08(9)	–	6.80	5.65

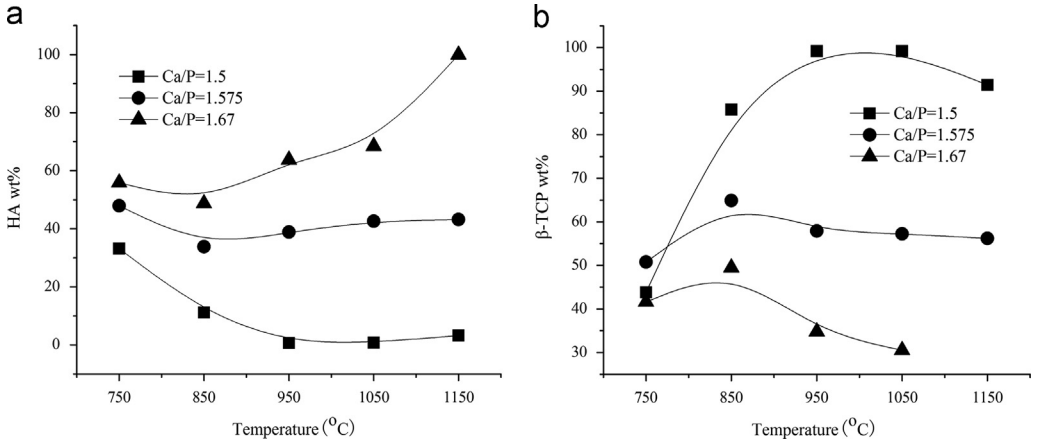

Fig. 7. Quantitative phases analyes extracted Rietveld refinement annealing at different temperatures (a) HA and (b) β-TCP.

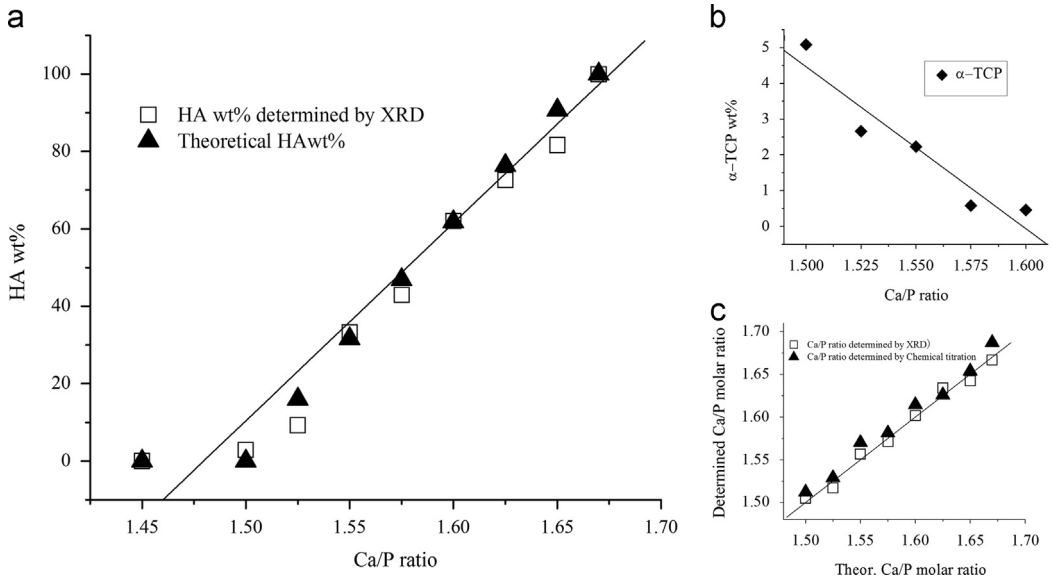

Fig. 8. Quantitative phases analysis extracted Rietveld refinement with different Ca/P ratios (a) HA wt% determined by XRD vs. theoretical HA wt%, (b) α-TCP wt%, (c) Comparison between theoretical Ca/P ratio (line) with that obtained by XRD(□) and chemical titration(▲).

attributed to the ν_4 vibration of the O–P–O mode. The peaks at 1640 and 1420cm^{-1} corresponded to absorbed water and vibration of CO_3^{2-} ions [50,51]. The bands at 3572, 1090, 630 and 571 cm^{-1} for HA structure formed with the Ca/P ratio reached 1.55, the bands at 1090 and 571 cm^{-1} corresponded to the ν_3 and ν_4 vibration, and the bands at 3572 and 630 cm^{-1} were attributed to the vibrations of OH^- ions. With increase of the Ca/P ratio,

Table 5
The lattice parameters extracted from Rietveld refinements.

Ca/P	T/°C	HA			β-TCP		
		a(Å)	*c*(Å)	*V*(Å3)	*a*(Å)	*c* (Å)	*V*(Å3)
1.45	1150	-	-	-	10.4344(8)	37.3897(5)	3525.5(8)
1.5	750	9.4075(7)	6.8705(5)	526.6(8)	10.4121(3)	37.3517(5)	3506.9(6)
	850	9.4277(1)	6.8835(5)	529.9(5)	10.4366(9)	37.4183(9)	3529.7(6)
	950	9.41(0)	6.879(0)	527.5(2)	10.4343(4)	37.4062(4)	3527(7)
	1050	9.41(0)	6.879(0)	527.5(2)	10.4350(7)	37.4037(3)	3527.2(1)
	1150	9.41(0)	6.879(0)	527.5(2)	10.4311(2)	37.3980(5)	3524(3)
1.525	1150	9.4186(4)	6.8801(9)	528.6(7)	10.4293(9)	37.3830(9)	3521.4(1)
1.55	1150	9.4165(9)	6.8788(1)	528.2(3)	10.4265(2)	37.3911(7)	3520.3(7)
1.575	750	9.4257(8)	6.8806(5)	529.4(3)	10.4311(6)	37.3876(8)	3523.1(5)
	850	9.4269(3)	6.8837(6)	529.8(7)	10.4380(9)	37.4123(1)	3530(1)
	950	9.4152(3)	6.8726(8)	527.6(1)	10.4227(1)	37.3572(4)	3514.5(2)
	1050	9.4122(6)	6.8752(6)	527.5(7)	10.4224(1)	37.3622(4)	3514.8(9)
	1150	9.4239(2)	6.8831(8)	529.4(9)	10.4339(2)	37.4090(7)	3527(6)
1.6	1150	9.4206(1)	6.8811(2)	528.9(7)	10.4231(8)	37.3987(2)	3518.7(9)
1.625	1150	9.4119(8)	6.8755(1)	527.5(6)	10.4155(7)	37.3437(6)	3508.4(1)
1.65	1150	9.4196(1)	6.8802(2)	528.7(9)	10.4218(4)	37.3845(8)	3516.5(8)
1.67	750	9.4260(6)	6.8821(8)	529.6(5)	10.4312(6)	37.3897(2)	3523.3(2)
	850	9.4254(6)	6.8845(6)	529.7(7)	10.4366(1)	37.4069(4)	3528.6(9)
	950	9.4286(6)	6.8821(6)	529.8(4)	10.4357(9)	37.4061(1)	3527.9(1)
	1050	9.4212(9)	6.8809(1)	528.9(2)	10.4285(8)	37.3841(4)	3521(7)
	1150	9.4224(4)	6.8828(2)	529.2(3)	–	–	

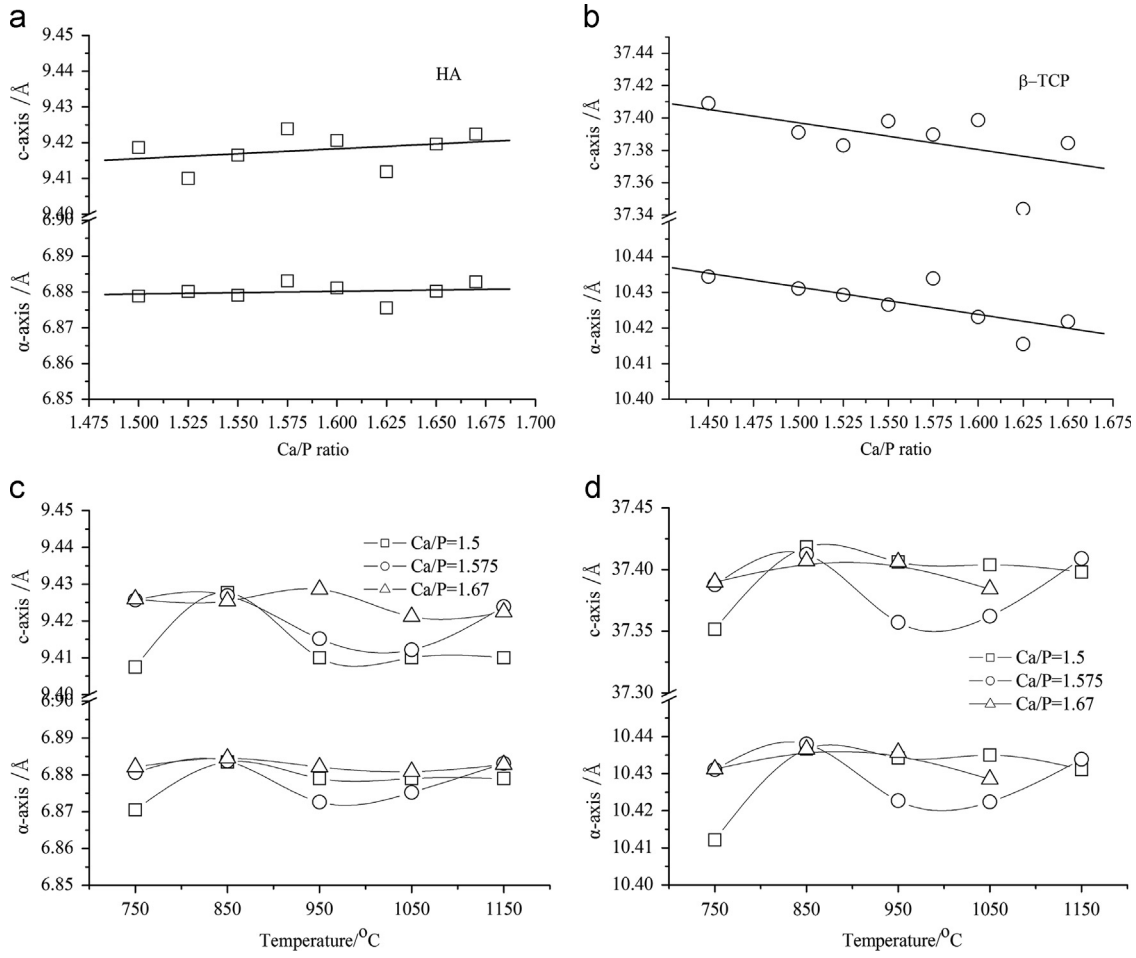

Fig. 9. The lattice parameter of HA and β-TCP (a) effect of Ca/P ratio on the lattice parameter of hydroxyapatite phase in compounds, (b) effect of Ca/P ratio on the lattice parameter of β-TCP phase in compounds, (c) effect of annealing temperature on the lattice parameter of hydroxyapatite phase in compounds, and (d) effect of annealing temperature on the lattice parameter of β-TCP phase in compounds.

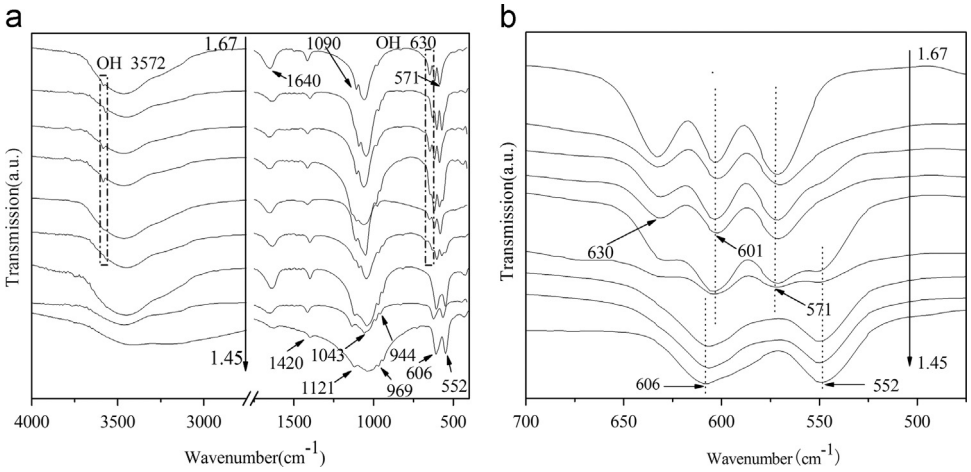

Fig. 10. (a) FTIR spectra of samples synthesized with different Ca/P ratios, (b) enlarged view of 700–400 cm^{-1}.

Table 6
IR frequencies of samples synthesized with different Ca/P ratio.

Band assignment	Frequency(cm^{-1})		Experimental Value(cm^{-1})								
	β-TCP	HA	1.45	1.5	1.525	1.55	1.575	1.6	1.625	1.65	1.67
PO_4^{3-}, ν_3 stretch.	1120		β	β	β	β					
		1082				H	H	H	H	H	H
	1042		β	β	β	β	β	β	β		
		1040								H	H
PO_4^{3-}, ν_1 stretch.	972		β	β	β	β	β	β			
		962							H	H	H
	945		β	β	β	β	β				
PO_4^{3-}, ν_1 stretch.4	606		β	β	β						
		601				H	H	H	H	H	H
		571				H	H	H	H	H	H
	552		β	β	β						
OH^-, stretch.		3572				H	H	H	H	H	H
OH^-, lib.		630				H	H	H	H	H	H

H and β corresponds to the bands of HA and β-TCP respectively.

the bands for β-TCP structure gradually disappeared. All of the bands corresponded to HA structure while the Ca/P ratio reached 1.65.

4. Conclusions

In this work we propose the utilization of a solution combustion method for the preparation of different calcium phosphates. Pure β-TCP is obtained with Ca/P=1.5 after annealing at 1050 °C, while HA phase is synthesized with Ca/P=1.67 after annealing at 1150 °C. The variation in the nominal Ca/P ratio provides a favorable way to control different proportions of BCP materials. In addition, thermal treatment with different temperatures also lead to the formation of biphasic materials in different proportions, the annealing temperature ranges from 850 °C to 1050 °C favored the formation of the β-TCP in this method. Finally, the relevance of phase transformation from β-TCP to HA is confirmed by the FTIR spectra. This method makes it possible to obtain single phase HA, β-TCP and BCP by regulating Ca/P ratio and annealing temperature.

Acknowledgment

This work was supported by Jiangsu Laboratory of Advanced Functional Materials.

References

[1] M. Jarcho, Calcium-phosphate ceramic as hard tissue prosthetics, Clinical Orthopaedics and Related Research 157 (1981) 259–278.
[2] N.O. Engin, A.C. Tas, Preparation of porous $Ca_{10}(PO_4)_6(OH)_2$ and $Ca_3(PO_4)_2$ bioceramics, Journal of the American Ceramic Society 83 (2000) 1581–1584.
[3] S. Kannan, S.I. Vieira, S.M. Olhero, P.M.C. Torres, S. Pina, O.A.B. Silva, Ferreira JMF. Synthesis, mechanical and biological characterization of ionic doped carbonated hydroxyapatite/β-tricalcium phosphate mixtures, Acta Biomater 7 (2011) 1835–1843.

[4] H. Yamasaki, H. Sakai, Osteogenic response to porous hydroxyapatite ceramics under the skin of dogs, Biomaterials 13 (5) (1992) 308–312.
[5] C.W. Song, T.W. Kim, D.H. Kim, H.H. Jin, K.H. Hwang, J.K. Lee, H.C. Park, S.Y. Yoon, In situ synthesis of silicon-substituted biphasic calcium phosphate and their performance in vitro, Journal of Physics and Chemistry of Solids 72 (2012) 39–45.
[6] J.D. Chen, Y.J. Wang, X.F. Chen, L. Ren, C. Lai, W. He, Q.Q.A. Zhang, Simple sol–gel technique for synthesis of nanostructured hydroxyapatite, tricalcium phosphate and biphasic powders, Materials Letters 65 (2011) 1923–1926.
[7] S.H. Kwon, Y.K. Jun, S.H. Hong, H.E. Kim, Synthesis and dissolution behavior of beta-TCP and HA/beta-TCP composite powders, Journal of the European Ceramic Society 23 (2003) 1039–1045.
[8] A. Piattelli, A. Scarano, C. Mangano, Clinical and histological aspects of biphasic calcium phosphate ceramic(BCP) used in connection with implant placement, Biomaterials 17 (1996) 1767–1770.
[9] S. Reynaud, E. Champion, A.D. Bernache, P. Thomas, Calcium phosphate apatites with variable Ca/P atomic ratio. I. Synthesis, characterization and thermal stability of powders, Biomaterials 23 (2002) 1065–1072.
[10] S. Yamada, D. Heymann, J.M. Bouler, G. Daculsi, Osteoclastic resorption of calcium phosphate ceramics with different hydroxyapatite with different hydroxyapatite/β-tricalcium phosphate ratios, Biomaterials 18 (1997) 1037–1041.
[11] O. Gauthier, J.M. Bouler, E. Aguado, R.Z. Legeros, P. Polet, G. Daculsi, Elaboration conditions influence physicochemical properties and in vivo bioactivity of macroporous biphasic calcium phosphate ceramics, Journal of Materials Science: Materials in Medicine 10 (1999) 199–204.
[12] M. Lukić, Z. Stojanović, S.D. Škapin, M.M. Kržmanc, M. Mitrić, S. Marković, D. Uskoković, Dense fine-grained biphasic calcium phoshate(BCP) bioceramics designed by two-step sintering, Journal of the European Ceramic Society 31 (2011) 19–27.
[13] Y.K. Jun, S.H. Hong, Y.M. Kong, Effect of co-precipitation on low-temperature sintering of biphasic calcium phosphate, Journal of the American Ceramic Society 89 (2006) 2295–2297.
[14] S. Kannan, I.A.F. Lemos, J.H.G. Rocha, J.M.F. Ferreira, Synthesis and characterization of magnesium substituted biphasic mixtures of controlled hydroxyapatite/β-tricalcium phosphate ratios, Journal of Solid State Chemistry 178 (2005) 3190–3196.
[15] X.D. Zhu, H.L. Zhang, H.S. Fan, W. Li, X.D. Zhang, Effect of phase composition and microstructure of calcium phosphate ceramic particles on protein absorption, Acta Biomaterialia 6 (2010) 1536–1541.
[16] B. Li, X.N. Chen, B. Guo, X.L. Wang, H.S. Fan, X.D. Zhang, Fabrication and cellular biocompatibility of porous carbonated biphasic calcium phosphate ceramics with a nanostructure, Acta Biomaterialia 5 (2009) 134–143.
[17] H. Borhane, Fellah, P. Layrolle, Sol–gel synthesis and characterization of macroporous calcium phosphate bioceramics containing microporosity, Acta Biomaterialia 5 (2009) 735–742.
[18] T.S. Kumar, I. Manjubala, J. Gunasekaran, Synthesis of carbonated calcium phosphate ceramics using microwave irradiation, Biomaterials 21 (2000) 1623–1629.
[19] I. Manjubala, M. Sivakumar, In-situ sythesis of biphasic calcium phosphate ceramics using microwave irradiation, Materials Chemistry and Physics 71 (2001) 272–278.
[20] J. Peña, M.V. Regí, Hydroxyapatite, tricalcium phosphate and biphasic matericals prepared by a liquid mix technique, Journal of the European Ceramic Society 23 (2003) 1687–1696.
[21] K. Itatani, T. Nishioka, S. Seike, F.S. Howell, A. Kishioka, M. Kinoshita, Sinterability of β-calcium orthophosphate powder prepared by spray pyrolysis, Journal of the American Ceramic Society 77 (1994) 801–805.
[22] F.H. Lin, C.J. Liao, K.S. Chen, J.S. Sun, C.Y. Lin, Preparation of β-TCP/HA biphasic ceramics with nature bone structure by heating boving cancellous bone with the addition of $(NH_4)_2HPO_4$, Journal of Biomedical Materials Research 51 (2000) 157–163.
[23] Y. Yang, Q.Q. Yao, X.M. Pu, Z.Q. Hou, Q.Q. Zhang, Biphasic calcium phosphate macroporous scaffolds derived from oyster shells for bone tissue engineering, Chemical Engineering Journal 173 (2011) 837–845.
[24] M.A. Aghayan, M.A. Rodríguez, Influence of fuels and combustion aids on solution combustion synthesis of bi-phasic calcium phosphates (BCP), Materials Science and Engineering C 32 (2012) 2464–2468.
[25] T. Singanahally, Aruna, Alexander S. Mukasyan, Combustion synthesis and nanomaterials, Current Opinion in Solid State and Materials Science 12 (2008) 44–50.
[26] A.C. Tas, Combustion synthesis of calcium phosphate bioceramic powders, Journal of the European Ceramic Society 20 (2000) 2389–2394.
[27] S. Sasikumar, R. Vijayaraghavan, Solution combustion synthesis of bioceramic calcium phosphates by single and mixed fuels—a comparative study, Ceramics International 44 (2008) 1373–1379.
[28] K. Samit, Nandi, B. Kundu, S.K. Ghosh, T.K. Mandal, S. Datta, D.K. De, D. Basu, Cefuroxime-impregnated calcium phosphates as an implantable delivery system in experimental osteomyelitis, Ceramics International 35 (2009) 1367–1376.
[29] Y.C. Han, S.P. Li, X.Y. Wang, X.M. Chen, Synthesis and sintering of nanocrystalline hydroxyapatite powders by citric acid sol–gel combustion method, Materials Research Bulletin 39 (2004) 25–32.
[30] H.K. Varma, S.N. Kalkura, R. Sivakumar, Polymeric precursor route for the preparation of calcium phosphate compounds, Ceramics International 24 (1998) 467–470.
[31] Y. Yuan, C.S. Liu, Y. Zhang, X.Q. Shan, Sol–gel auto-combustion synthesis of hydroxyapatite nanotubes array in porous alumina template, Materials Chemistry and Physics 112 (2008) 275–280.
[32] M. Ferrari, L. Lutterotti, Method for the simultaneous determination of anisotropic residual stresses and texture by X-ray diffraction, Journal of Applied Physics 76 (1994) 7246–7255.
[33] P. Sahu, M. De, Zdujić, Microstructural characterization of the evoluted phases of ball-milled α-Fe_2O_3 powder in air and oxygen atmosphere by Rietveld analysis, Materials Chemistry and Physics (2003) 864–876.
[34] J.R. Martínez, S.P. Sánchez, G.O. Zarzosa, F. Ruiz, Y. Chumakov, Rietveld refinement of amorphous SiO_2 prepared via sol–gel method, Materials Letters 60 (2006) 3526–3529.
[36] N.C. Popa, D. Balzar, An analytical approximation for a size-broadened profile given by the lognormal and gamma distributions, Journal of Applied Crystallography 35 (2002) 338–346.
[37] L. Ge, W. Zhou, R. Ran, Z.P. Shao, S.M. Liu, Facile auto-combustion synthesis of $La_{0.6}Sr_{0.4}Co_{0.2}Fe_{0.8}O_{3-\delta}$ (LSCF) perovskite via a modified complexing sol–gel process with NH_4NO_3 as combustion aid, Journal of Alloys and Compounds 450 (2008) 323–329.
[38] L. Ge, R. Ran, Z.P. Shao, H.Z. Zhu, S.M. Liu, Low-temperature synthesis of $La_{0.6}Sr_{0.4}Co_{0.2}Fe_{0.8}O_{3-\delta}$perovskite via asymmetric sol–gel process and catalytic auto-combustion, Ceramics International 35 (2009) 2809–2815.
[39] K.S. TenHuisen, P.W. Brown, Phase evolution during the formation of α-tricalcium phosphate, Journal of the American Ceramic Society 82 (1999) 2813–2818.
[40] A.T. Saenger, W.F. Kuhs, Structural disorder in hydroxyapatite, Z Kristallogr 199 (1992) 123–148.
[41] M. Yashima, A. Sakai, T. Kamiyama, A. Hoshikawa, Crystal structure analysis of beta-tricalcium phosphate $Ca_3(P\ O_4)_2$ by neutron powder diffraction, Journal of Solid State Chemistry 175 (2003) 272–277.
[42] M. Mathew, L.W. Schroeder, B. Dickens, W.E. Brown, The crystal structure of alpha-$Ca_3(P\ O_4)_2$, Acta Crystallographica Section B 33 (1977) 1325–1333.
[43] S. Boudin, A. Grandin, M.M. Borel, A. Leclaire, B. Raveau, Redetermination of the beta-$Ca_2P_2O_7$ structure, Acta Crystallographica Section C 49 (1993) 2062–2064.
[44] S.A. Markgraf, R.J. Reeder, High-temperature structure refinements of calcite and magnesite, American Mineralogist 70 (1985) 590–600.
[45] D.K. Smith, H.R. Leider, Low-temperature thermal expansion of Li H, MgO and CaO, Journal of Applied Crystallography 1 (1968) 246–249.
[46] N. Kivrak, A.C. Tas, Synthesis of calcium hydroxyapatite–tricalcium phosphate (HA–TCP) composite bioceramic powders and their sintering behavior, Journal of the American Ceramic Society 81 (1998) 2245–2252.
[47] Q.J. He, Z.L. Huang, X.K. Cheng, J. Yu, Thermal stability of porous A-type carbonated hydroxyapatite spheres, Materials Letters 62 (2008) 539–542.

[48] B.O. Fowler, Infrared studies of apatites, vibrational assignments for calcium, strontium and barium hydroxyapatites utilizing isotopic substitution, Inorganic Chemistry 13 (1974) 194–207.
[49] A. Jillavenkatesa, R.A. Condrate, The infrared and raman spectra of β and α-tricalcium phosphate $Ca_3(PO4)_2$, Spectroscopy Letters 31 (1998) 1619–1634.
[50] T.S.S. Kumar, I. Manjubala, J. Gunasekaran, Synthesis of Carbonated calcium phosphate ceramics using microwave irradiation, Biomaterials 21 (2000) 1623–1629.
[51] R.N. Panda, M.F. Hsieh, R.J. Chung, T.S. Chin, X.R.D. FTIR, SEM and solid state NMR investigations of carbonate-containing hydroxyapatite nano-particles synthesized by hydroxide–gel technique, Journal of Physics and Chemistry of Solids 64 (2003) 193–199.